

Iodine-129 Mössbauer spectroscopy: Probing the molecular orientation in liquid crystals*

M. J. Potasek,[†] P. G. Debrunner, and G. DePasquali

Physics Department, University of Illinois at Urbana-Champaign, Urbana, Illinois 61801

(Received 5 May 1975)

A series of ^{129}I Mössbauer measurements have been completed on 4-*n*-hexoxybenzylidene-4'- ^{129}I iodoaniline dissolved in the liquid crystal 4-*n*-hexoxybenzylidene-4'-*n*-propylaniline. Ordered solute "monocrystals" were produced by orienting the samples in an external magnetic field. The sample exhibited three liquid-crystalline phases: nematic, smectic *A*, and smectic *H*. Analysis of the ^{129}I Mössbauer spectra gave a value of $50 \pm 4^\circ$ for the smectic-*H* tilt angle.

I. LIQUID CRYSTALS AND MÖSSBAUER SPECTROSCOPY

Materials exhibiting phases intermediate between an isotropic liquid and a solid are called liquid crystals (LC). These phases have properties characteristic of both the isotropic liquid and the three-dimensional solid. There are two main classes of LC: (a) Thermotropic—a one-component system whose phase transitions occur as a function of temperature. These phases exhibit various degrees of order. (b) Lyotropic—usually a two-component aqueous system whose phase transitions occur as a function of both solute concentration and temperature. The lyotropic LC state is essential for many biological functions. One significant lyotropic LC system is the myelin sheath which surrounds the nerve axons.¹ This sheath is vital for the rapid transmission of electrical impulses in nerves. Phospholipids which form lyotropic LCs in an aqueous medium are important components of all cell membranes. Certain difficulties encountered in the study of complex cell membranes can be avoided by the use of an aqueous phospholipid model membrane. These aqueous phospholipids form complex lyotropic LC phases.² The molecular-order characteristic of the membranes is vital to the functions of the cell.

Various techniques³ have been used to investigate the molecular order in LC. A relatively new tool in this area is Mössbauer spectroscopy (MB). An advantage of this technique relative to some of the other probes used to investigate the molecular order in LC, is that MB is sensitive to only certain nuclides, thereby providing one with a powerful method for the investigation of complex LC systems. While nuclear-magnetic-resonance techniques can be used to study orientation in LCs, one can obtain, in principle, more detailed information about the orientation distribution function of the LC from MB. (See Sec. IV.) While time-consuming x-ray analysis can provide more

detailed structural data, initial indications of molecular order can be obtained from a few MB measurements. Molecules which cannot be crystallized for x-ray analysis or are difficult to order can often be placed in a LC matrix and ordered. This order can then be investigated by MB.

Of the possible MB nuclides only ^{57}Fe ,⁴⁻⁷ ^{119}Sn ,⁸ and ^{129}I ,⁹ have been used in LC studies. (See Sec. II.) Low temperatures are used for ^{129}I MB studies. However, in very ordered LC states (such as the smectic-*H* state, which we study here) the molecular order at low temperatures is essentially the same as at the LC temperature. Other MB nuclides such as ^{57}Fe and ^{119}Sn can be studied at high temperatures. However, only iodine can be incorporated into molecules that are very similar to LC. In a few cases the resultant compound is still a LC.^{9,10} Therefore, ^{129}I was selected as the MB probe.

^{129}I MB studies of phospholipid systems have been initiated in this laboratory; however, a complete analysis of the spectra is in progress.¹¹ Since there are several nonequivalent ^{129}I sites in this system which give rise to numerous overlapping absorption lines, it was decided to investigate the molecular order of a thermotropic LC containing only one ^{129}I site. A mixture of 4-*n*-hexoxybenzylidene-4'- ^{129}I iodoaniline (HB ^{129}IA), 20% by weight, dissolved in the LC 4-*n*-hexoxybenzylidene-4'-*n*-propylaniline (HBPA) was used in this study. The reasons for selecting this LC mixture are discussed in the Secs. II and V. This LC mixture will be referred to as the sample.

The structure formulas of HB ^{129}IA and HBPA are shown in Fig. 1. The sample exhibits three thermotropic LC phases: nematic, smectic *A*, and smectic *H*. The molecular order of these phases is shown in Fig. 2.

Differential scanning calorimetry (DSC) and microscope studies were used to determine the phase transitions of the sample, which are

solid $\xrightarrow{24^\circ\text{C}}$ smectic *H* $\xrightarrow{54^\circ\text{C}}$ unknown $\xrightarrow{68.5^\circ\text{C}}$ smectic *A* $\xrightarrow{77.3^\circ\text{C}}$ nematic $\xrightarrow{93.3^\circ\text{C}}$ isotropic liquid.

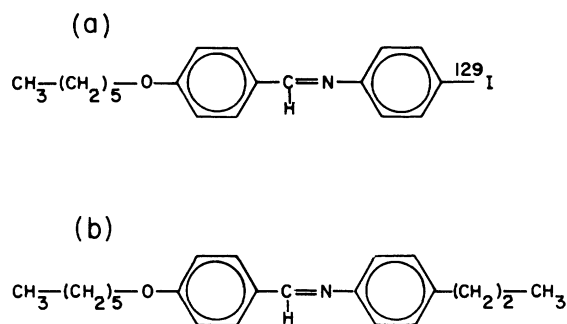


FIG. 1. The chemical structure formulas for (a) 4-*n*-hexoxybenzylidene-4'-¹²⁹I-iodoaniline and (b) 4-*n*-hexoxybenzylidene-4'-*n*-propylaniline.

A description of the molecular order of each of the three LC phases is presented next. (See Fig. 2.)

Nematic: The least-ordered LC phase is the nematic. The long axes of the molecules lie parallel to an axis in space, but the centers of mass of the molecules are randomly distributed. The molecules are free to rotate about their long axes. Maier and Saupe¹² introduced a molecular model based on dipole-dipole dispersion forces and solved this model in the mean field approximation. In this approximation they introduced the orienta-

tional order parameter $S' = \langle \frac{3}{2} \cos^2 \beta - \frac{1}{2} \rangle$, where β is the angle between the long axis of a molecule and a preferred axis in space.

Smectic A: Kobayashi¹³ and McMillan¹⁴ have independently introduced a microscopic theory for the smectic-*A* phase. This phase is characterized by its layered structure. The long axes of the molecules are aligned and the centers of mass of the molecules are arranged on a plane. However, the molecules are free to rotate about their long axes.

Smectic H: This recently discovered phase is essentially a three-dimensional ordered structure. X-ray-diffraction studies on the smectic-*H* phase of 4-butyloxybenzal-4-ethylaniline¹⁵ (BEA) showed that the molecules are arranged in layers but the long axes of the molecules are tilted at an angle of 56.2° with respect to the planes of the layers. The neighboring layers are not free to slide over one another. The packing of the molecules within a plane is hexagonal. Meyer and McMillan¹⁶ have recently proposed a microscopic theory for the smectic-*H* phase which is an extension of McMillan's^{14,17} earlier theories.

The smectic-*H* phase has been shown to supercool below 77 K,⁸ thus making it an excellent phase for low-temperature ¹²⁹I MB spectroscopy.

Information concerning the orientation of the sample is contained in the intensities of the MB lines. Since the recoilless fraction also alters the MB intensities, it has been incorporated into a general formalism to describe the orientation (see Sec. IV). The MB spectra of the oriented solute molecules (HB ¹²⁹IA) in the LC host (HBPA) were analyzed using a nonlinear least-squares-fitting program of theoretical spectra to the data. In addition to the orientation parameters, we have evaluated the chemical iodine bonding parameters (from the MB line positions) of HB ¹²⁹IA and have related them to the corresponding parameters for several similar compounds.

II. EXPERIMENTAL METHODS

MB spectroscopy of ⁵⁷Fe,⁴⁻⁷ ¹¹⁹Sn,⁸ and ¹²⁹I,⁹ has been used to study orientation in LC. Using 1,1'-diacetylferrocene, DAF, ⁵⁷Fe dissolved in the LC, 4,4'-bis(heptyloxy)-azoxybenzene, Uhrich *et al.*⁴ found some orientation of the solute molecule, DAF, when the LC was oriented in the nematic phase by an external magnetic field. These ⁵⁷Fe MB measurements were done in the temperature range from 298–367 K. The first direct MB study on a LC was by Potasek *et al.*⁹ using ¹²⁹I incorporated into the LC, 6-heptyloxy-5-¹²⁹iodo-2-naphthoic acid (H¹²⁹INA). Since ¹²⁹I measurements must be made at low temperatures, the order of

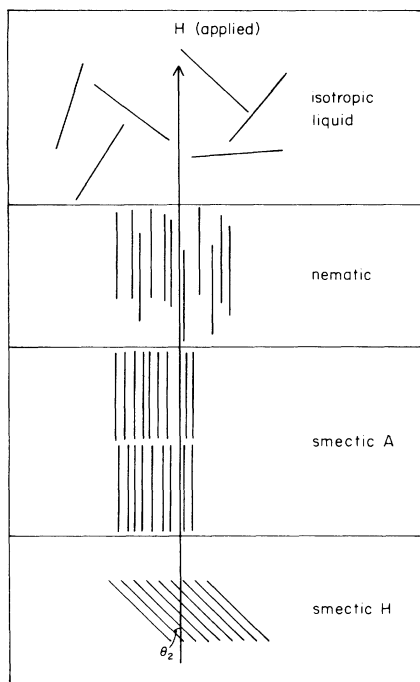


FIG. 2. Molecular order of the isotropic liquid, nematic, smectic *A*, and smectic *H* phases is shown. The straight lines represent the long axes of the liquid-crystal molecules.

the magnetically aligned nematic phase of $H^{129}\text{INA}$ (the nematic-isotropic liquid phase transition of $H^{129}\text{INA}$ occurs at 189°C) had to be quenched down to 55 K. While the LC showed substantial orientation, it was desirable to use a system in which (a) the LC phases occurred at a lower temperature, (b) there existed a nematic phase which is necessary for bulk orientation of the LC in an external magnetic field, (c) there existed low-temperature smectic phases which are more viscous than the nematic phase and convenient for low-temperature MB spectroscopy, and (d) there was significant supercooling of the smectic LC phases. These conditions are satisfied by HBPA. (At present, there is no iodine-containing LC which satisfies these conditions.)

^{119}Sn MB measurements of triethyltin palmitate (3EtSnPalm) dissolved in HBPA were made by Uhrich *et al.*⁸ Their MB measurements, which were made in the supercooled smectic- H phase (77 K) of HBPA, showed that the solute molecule, 3EtSnPalm, was oriented by the LC, HBPA. However, they were not able to measure the smectic- H tilt angle of HBPA.

Since the LC is used to orient the MB probe molecule, it is desirable to select a probe molecule that is more similar to HBPA than 3EtSnPalm is. Replacement of the propyl group of HBPA by iodine yields HBIA whose structure is very similar to that of HBPA. Unfortunately, HBIA does not exhibit the necessary LC phases, but a mixture of HBIA in HBPA does. (See Sec. V.)

The MB sample ($H^{129}\text{IA}$, 20% by weight, dissolved in HBPA) was oriented in the nematic phase by an external magnetic field ($H = 6.8 \pm 0.3$ kG). In this phase the long axes of the LC molecules align along H as shown in Fig. 1. Upon cooling to the smectic- A phase, in the presence of H , the long axes of the molecules remain aligned along H but attain a layered structure. However, when the sample cools to the smectic- H phase, the molecules lie on a cone about the direction of the external magnetic field and attain the characteristic tilt angle as shown in Fig. 2. In the smectic- H phase the molecules retain their order even when the sample is not in the external magnetic field. Consequently, the oriented sample can easily be mounted in the MB cryostat. The procedure for orienting the sample and the experimental MB arrangement are discussed next.

An oriented MB sample was prepared in the following way. A $\frac{3}{8}$ -in.-i.d. Teflon, disk-shaped sample holder containing 50 mg of the LC mixture (sample thickness ≈ 0.5 mm) was mounted in the copper heating oven. (See Fig. 3.) Nichrome wire which was wound tightly around the copper heating oven and then connected to a Variac was

used to heat the sample. Sample temperatures were measured to within $\pm 0.1^\circ\text{C}$ using a mercury thermometer which was rigidly attached to the sample holder with copper tape. The heating oven was mounted in a $1\frac{3}{8}$ in. gap of a Varian model V-4004 electromagnet equipped with a model V-2300A power supply. An angle θ_1 , the angle between the normal to the sample holder and H , was selected by rotating the center tube. (See Fig. 3.) After the sample chamber was evacuated and filled with dry helium gas, the sample was heated to the isotropic liquid phase and allowed to cool slowly to the nematic phase in the presence of the external magnetic field. It was maintained in the nematic phase for 35 min. Then, with the magnetic field applied, the sample was cooled to room temperature. The heating and cooling rate was $0.2^\circ\text{C}/\text{min}$. The sample holder was removed from the oven and slowly submerged in liquid nitrogen.

This same sample holder was mounted on the axis of the MB velocity drive with the normal to the sample holder along the direction of propagation of the gamma rays. For the MB measurements, the standard transmission geometry and a Hewlett-Packard multichannel analyzer were used.

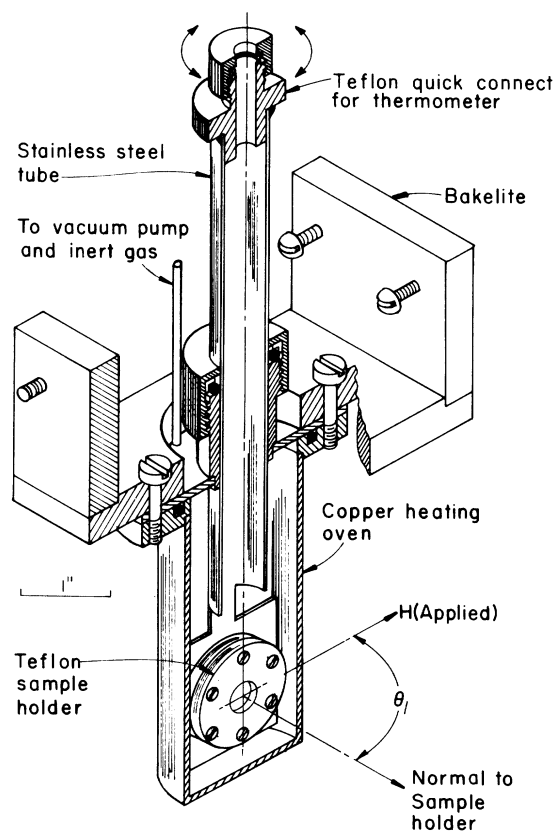


Fig. 3. Apparatus used for orienting the samples.

The velocity drive was of the constant-acceleration type. Both the MB source ($\text{Zn}^{129\text{m}}\text{Te}$) and the LC absorber were maintained at liquid-helium temperature during the MB measurements.

III. SOURCE AND ABSORBER PREPARATION

The single-line MB source was $\text{Zn}^{129\text{m}}\text{Te}$. The isotopically pure elements ^{66}Zn and ^{128}Te were obtained from Oak Ridge National Laboratory. 75 mg of $^{66}\text{Zn}^{128}\text{Te}$ were irradiated at a neutron flux of 1.75×10^{14} neutrons $\text{cm}^{-2}\text{sec}^{-1}$ for 30 days at the University of Missouri reactor facilities. The active compound $\text{Zn}^{129\text{m}}\text{Te}$ ($T_{1/2} = 33$ days) was sealed in an aluminum MB source holder.

The MB absorber consisted of HB^{129}IA , 20% by weight, dissolved in the LC, HBPA. The LC was synthesized by the following procedure.¹⁸ 4-*n*-hexoxybenzaldehyde (HB) and *p*-propylaniline (PA) were obtained from Eastman Kodak Co. 8.1 g of HB, 5.7 ml of PA, and 32 ml of ethanol were refluxed for 1 h in a three-neck 100 ml flask, fitted with a thermometer and a reflux condenser. The hot contents were transferred to a 100 ml beaker and allowed to cool to room temperature. The supernatant was decanted and the white crystals were dried on filter paper. The crystals were recrystallized from ethanol three times. The purity was determined by chemical analysis, differential scanning calorimetry (DSC), and microscope studies (C: found, 81.48; calculated, 81.73; H: found, 9.13; calculated, 8.97; N: found, 4.33; calculated, 4.33). DSC and microscope studies are reported in Sec. V.

HB^{129}IA was synthesized using a modification of the method by Bradfield *et al.*¹⁹ ^{129}I , in basic NaSO_3 solution, was purchased from Oak Ridge National Laboratory. The basic solution containing 154 mg of ^{129}I was evaporated to dryness, then dissolved in ethanol. The insoluble sulfite was filtered off. Evaporation of the ethanol left Na^{129}I which was dissolved in 1 ml of acetic acid. The Na^{129}I solution was added dropwise to 300 mg of chloramine *T* dissolved in 2 ml of acetic acid. The resulting solution was added to 0.11 ml of freshly distilled aniline which was diluted with 1 ml of acetic acid. The mixture was allowed to stand for 10 min and then was transferred to a separatory funnel. The resulting *p*- $^{129}\text{iodoaniline}$ (P^{129}IA) was diluted with 6 ml water and extracted with 20 ml of ether. The ether phase was washed with water, sodiumthiosulfate, and again with water. The ether was then evaporated and the residue was dissolved in ethanol. The resulting solution was boiled for 5 min with activated charcoal, filtered and the solid was allowed to crystallize. This alcohol purification was repeated

three times yielding 186 mg of P^{129}IA . 20 mg was set aside for MB measurements; the remaining 166 mg of P^{129}IA and 157 mg of HB were dissolved in 3 ml of ethanol. The mixture was refluxed for 2 h and then allowed to stand for 2 h at room temperature. The resulting crystals of HB^{129}IA were filtered, washed with ethanol, and dried in vacuo. The yield was 37 mg. The purity was determined by chemical analysis (C: found, 56.25; calculated, 56.02; H: found, 5.64; calculated, 5.41; N: found, 3.35; calculated, 3.43; I: found, 30.05; calculated, 31.70).

20.4 mg of HB^{129}IA and 102 mg of HBPA was dissolved in 3–5 ml of ethanol. The solution was warmed slightly to about 30°C. Then the ethanol was evaporated under dry argon and 50 mg of the solid material was transferred to a Teflon sample holder. (See Fig. 3.)

IV. ANALYSIS OF THE DATA

The MB spectra (see Figs. 4 and 5) show resolved splitting as a result of the nuclear quad-

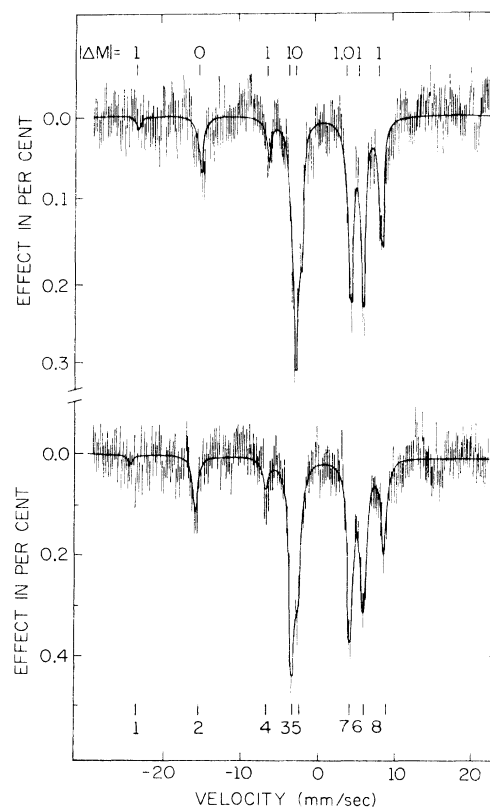


FIG. 4. Mössbauer spectra of HB^{129}IA dissolved in HBPA. The upper spectrum is an oriented sample with $\theta_1 = 0^\circ$. The lower spectrum is a random powder sample of HB^{129}IA . The numbers beneath the lower spectrum correspond to the transitions shown in Fig. 4.

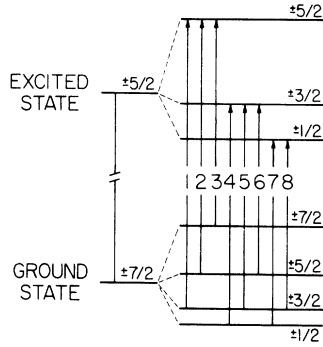


FIG. 5. Mössbauer nuclear transitions of ^{129}I for an axially symmetric electric-field-gradient tensor.

rupole interaction²⁰

$$\mathcal{K} = \frac{e^2 q Q}{4I(2I-1)} [3I_x^2 - I(I+1) + \eta(I_x^2 - I_y^2)]. \quad (1)$$

Here $e^2 q Q$ is the nuclear quadrupole coupling constant, I is the nuclear spin with components I_i , $i = x, y, z$, and η is the asymmetry parameter.

Since least-squares computer fits to the data give $\eta = 0.06 \pm 0.03$ (Table I), an axially symmetric electric-field-gradient tensor (EFG) is assumed for the calculation of the transition probabilities.

The MB transition probability for a single-line source can be written²¹

$$I(\nu) = N \int d\theta_2 \Theta(\theta_2) \mathcal{F}(\theta_3) \times \sum_{\substack{m_g, m_g \\ s = \pm 1}} L_{m_g}^{m_g}(\nu) |\langle \hat{k}_s I_g m_g | H | I_g m_g \rangle|^2, \quad (2)$$

where

$$L_{m_g}^{m_g}(\nu) = \frac{(\frac{1}{2}\Gamma)^2}{[E_{m_g}^{m_g}(\eta) - (v/c)E_\gamma]^2 + (\frac{1}{2}\Gamma)^2},$$

$$\frac{1}{2}\Gamma = \frac{1}{2}\Gamma(\text{source}) + \frac{1}{2}\Gamma(\text{absorber}).$$

Here I_g (I_e) is the nuclear spin in the ground (excited) state with z component m_g (m_e), $E_{m_g}^{m_g}(\eta)$ are the transition energies as defined by Shenoy and Dunlap,²² v is the relative velocity of the source and absorber, Γ is the full width at half-maximum, k is the direction of propagation of the γ ray with polarization s , N is a constant, and $E_\gamma = 27.8$ keV.

Figure 6 defines the angles θ_1 , θ_2 , and θ_3 , where θ_1 is the angle between the incident γ -ray and the direction of the external magnetic field. (This is the same angle θ_1 shown in Fig. 3, since the normal to the sample holder is along the incident γ ray in the experimental MB arrangement.) θ_2 is the angle between the z axis (V_{zz}) of the principal axes of the EFG and H . (It is assumed that V_{zz}

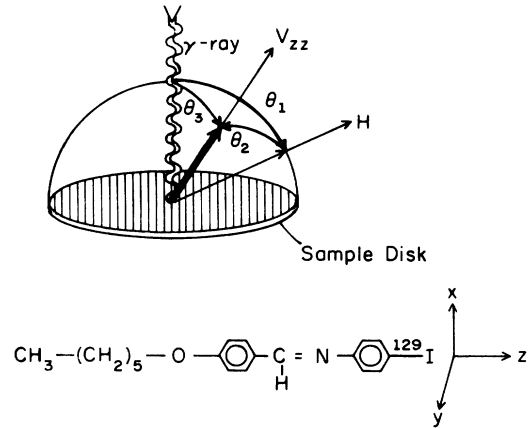


FIG. 6. Angles used for the calculations of the Mössbauer spectra. The lower part of the figure shows the chemical structure formula of HB ^{129}IA . To the right of the structure formula are the principal axes of the electric field gradient tensor.

lies along the long axis of HB ^{129}IA . The justification for this assumption is discussed in Sec. V B.) θ_3 is the angle between the incident γ ray and V_{zz} , and is measured by MB spectroscopy. θ_1 is selected in the laboratory as discussed in Sec. II.

$\Theta(\theta_2)$ is the probability that V_{zz} makes an angle θ_2 with respect to H . The method of Potasek *et al.*⁹ is adopted to describe the orientation. Since the radiation is a magnetic dipole ($M1$), it is convenient to expand $\Theta(\theta_2)$ in spherical harmonics,

$$\Theta(\theta_2) = \sum_D A_{D0} Y_{D0}(\theta_2). \quad (3)$$

Information about the orientation of the sample is contained in the relative intensities of the MB lines. Since the anisotropic recoilless fraction $\mathcal{F}(\theta_3)$ also alters the intensities, it is included in this calculation. Using the result of Goldanskii *et al.*²³ $\mathcal{F}(\theta_3)$ can be written

$$\mathcal{F}(\theta_3) = \exp(-k^2 \langle x_\perp^2 \rangle + S \cos^2 \theta_3), \quad (4)$$

where $S = k^2(\langle x_\perp^2 \rangle - \langle x_\parallel^2 \rangle)$, $k = 2\pi/\lambda$, λ is the wavelength of the γ ray, and $\langle x_\perp^2 \rangle$ ($\langle x_\parallel^2 \rangle$) is the mean-square vibrational amplitude of the nucleus perpendicular (parallel) to V_{zz} . For convenience, $\mathcal{F}(\theta_3)$ is expanded in spherical harmonics

$$\mathcal{F}(\theta_3) = \exp(-k^2 \langle x_\perp^2 \rangle) \sum_E B_{E0} Y_{E0}(\theta_3), \quad (5)$$

$$B_{E0} = 2\pi \sum_{l=0}^{S'} \frac{S^l}{l!} \int_{-1}^1 (\cos \theta_3)^{2l} Y_{E0}(\theta_3) d(\cos \theta_3).$$

Finally, combining Eqs. (2), (3), and (5), the MB intensity can be written

$$I(v) = N' \sum_{m_e, m_g} L_{m_g}^{m_e}(v) \begin{pmatrix} I_g & 1 & I_e \\ m_g & \Delta M & -m_e \end{pmatrix}^2 \sum_D \frac{A_{D0} Y_{D0}(\theta_1)}{(2D+1)^{1/2}} \left[B_{D0} + \frac{3(\Delta M)^2 - 2}{2} \sum_E [(2E+1)(2D+1)]^{1/2} B_{E0} \begin{pmatrix} D & 2 & E \\ 0 & 0 & 0 \end{pmatrix}^2 \right], \quad (6)$$

where $\Delta M = m_e - m_g$. When the recoilless fraction is isotropic the series in Eq. (6) reduces to an expression with $D = 0, 2$. The presence of $\mathfrak{F}(\theta_3)$ allows one to probe higher-order even expansion coefficients in the distribution function, Eq. (3).

It is convenient to rewrite Eq. (6) in the form

$$I(v) = N_1 \sum_{m_e, m_g} L_{m_g}^{m_e}(v) \begin{pmatrix} I_g & 1 & I_e \\ m_g & \Delta M & -m_e \end{pmatrix}^2 \times [\delta_{|\Delta M|, 1} + \mathfrak{M} \delta_{\Delta M, 0}]. \quad (7)$$

Here \mathfrak{M} is the average of the normalized $\Delta M = 0$ transition intensities divided by the average of the normalized $\Delta M = \pm 1$ transition intensities. The observed intensity divided by the transition probability for the line is the normalized intensity. The parameter \mathfrak{M} contains all of the information about the orientation parameters, A_{D0} .

If \mathfrak{M} is obtained for a random powder, then

$$\mathfrak{M} = (\sqrt{5} - B_{20}/B_{00})(\sqrt{5} + B_{20}/2B_{00})^{-1} \quad (8)$$

from which the value of B_{20}/B_{00} can be obtained. Then from Eq. (5) all of the B_{E0} terms can be determined. As a result the only unknowns in Eq.

(7) are the orientation parameters A_{D0} which can be determined from measurements of \mathfrak{M} as a function of θ_1 .

The form of Eq. (7) is convenient for least-squares computer fitting. The background, intensity, isomer shift relative to the Zn 129m Te source, e^2qQ , η , and \mathfrak{M} were the parameters varied in a computer fit of the theoretical spectrum given by Eq. (7) to the data. The least-squares-fitting program was written by Chrisman and Tumolillo²⁴ and later modified by Groves.²⁵ It incorporates the linear-approximation method for η written by Shenoy and Dunlap.²²

V. RESULTS AND DISCUSSION

A. Differential scanning calorimetry and microscope studies

DSC measurements were made on a DuPont 900 thermal analyzer. A standard polarizing microscope equipped with a Mettler FP5 programmable microscope heating stage was used to determine the LC phases.

The phase transitions of a recrystallized sample of HBPA are



in agreement with the results of Uhrich *et al.*⁸

Addition of the solute molecule, HBIA alters the phase transitions of the LC as shown in Fig. 7. As the concentration of HBIA increases, the ranges of the smectic-*H* and the nematic phases decrease while that of the smectic-*A* phase increases. DSC measurements show the presence of an unknown phase which could not be identified microscopically. McMillan has found a similar result for terephthal-bisbutylaniline.²⁶

Bulk orientation of the sample is achieved in the nematic phase in the presence of an external magnetic field. For a 30% by weight concentration of HBIA in HBPA the range of the nematic phase is too short to get reliable orientation. However, it is necessary for MB measurements to maximize the amount of ^{129}I in the sample. A 20%-by-weight concentration of HBIA in HBPA fulfills both conditions.

B. Chemical parameters

MB spectroscopy is sensitive to changes in the valence electrons of iodine and reflects the nature

of the iodine bond. The iodine anion (I^-) has a $5s^2 5p^6$ configuration.

We have measured the MB spectra of HB ^{129}IA as a solid, in a frozen ethanol glass (8 mM), and in a 20%-by-weight concentration in the LC, HBPA. The MB parameters are listed in Table I. For comparison, Table I contains the MB parameters of HB ^{129}IA and several similar compounds, $P^{129}\text{IA}$, $H^{129}\text{IA}$,⁹ L - α -thyroxine (T_4),²⁷ and diiodotyrosine ($D^{129}\text{IT}$).²⁷ The sign of e^2qQ (see Table I) is negative for all the compounds, indicating a greater $5p$ electron density in the x and y directions than in the z direction.²⁸ Furthermore the electric field gradient is nearly axially symmetric ($\eta \approx 0$) for all the compounds. The MB parameters of $P^{129}\text{IA}$ and HB ^{129}IA are indistinguishable from one another and similar to those of the other compounds listed in Table I.

For further analysis of the bonding in HB ^{129}IA , expressions from Greenwood and Gibb²⁸ are used. The empirical formula, Eq. (9) relates the isomer shift relative to a ZnTe source ($^{129}\delta_{\text{ZnTe}}$) to the iodine electron charge density

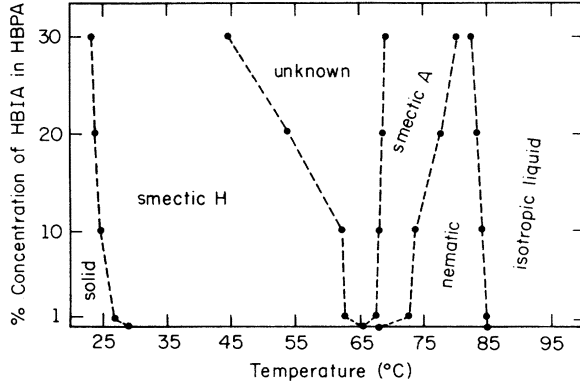


FIG. 7. Differential scanning calorimetry measurements as a function of the percent concentration (by weight) of HBIA in HBPA.

$${}^{129}\delta_{z\text{nTe}} = -8.2h_s + 1.5h_p - 0.54 \text{ mm/sec.} \quad (9)$$

Here $h_s(h_p)$ is the number of $5s(5p)$ electron holes in the $5s^25p^6$ configuration.

Considering an admixture of $5p \sigma$ and $5p \pi$ bonding, the population of electrons in the $5p_x$ and $5p_y$ orbitals can be expressed²⁸

$$U_x = U_z + U_p(1 + \frac{1}{3}\eta), \quad U_y = U_z + U_p(1 - \frac{1}{3}\eta), \quad (10)$$

where U_z is the population of electrons in the $5p_z$ orbital and U_p is the ratio of the molecular quadrupole coupling constant to the atomic quadrupole coupling constant,

$$U_p = -e^2q_{\text{mol}}Q/e^2q_{\text{at}}Q. \quad (11)$$

The quadrupole coupling constant for atomic ${}^{127}\text{iodine}$ is 2293 MHz .²⁸

Using the limits $0 \leq U_i \leq 2$, $i = (x, y, z)$ in Eqs. (9)–(11) results in the minimum value of h_s ($h_s = 0.07$) for HB ${}^{129}\text{IA}$. From Eqs. (10) and (11), $U_x = 2.00$, $U_y = 1.96$, and $U_z = 1.19$ are obtained. These values were computed from the MB parameters for the 20%-by-weight concentration of HB ${}^{129}\text{IA}$ in HBPA. (See Table I.)

The iodine in HB ${}^{129}\text{IA}$ forms primarily a $5p_z \sigma$ bond. The z axis is along the iodine-carbon bond. Since the iodine, which is in the para-position of the benzene ring in HB ${}^{129}\text{IA}$ forms a σ bond, it is reasonable to assume that V_{zz} is along the long axis of the molecule. (See Fig. 6.)

C. Orientation Parameters

In order to evaluate the distribution function of the sample, we determined \mathfrak{M} for a random powder of HB ${}^{129}\text{IA}$. Analysis of the MB spectrum, as described in Sec. IV, gave a value of $\mathfrak{M} = 0.96 \pm 0.04$. Then from Eqs. (5) and (8), the values of $B_{20}/B_{00} = 0.061$, $B_{40}/B_{00} = 1.58 \times 10^{-3}$, and $S = 0.2$ are obtained. Since $\mathfrak{M} \approx 1$, the recoilless fraction is nearly isotropic. As a result, the distribution function, given by Eq. (3), can be determined to only second order. Using Eqs. (6) and (7) the value of \mathfrak{M} becomes

$$\mathfrak{M} = \frac{1 - (1/\sqrt{5})(B_{20}/B_{00}) + \alpha(-1/\sqrt{5} + \frac{1}{7}B_{20}/B_{00} - 2\sqrt{\frac{9}{245}}B_{40}/B_{00})}{1 + (2\sqrt{5})^{-1}B_{20}/B_{00} + \alpha[(2\sqrt{5})^{-1} + \frac{10}{7}B_{20}/B_{00} + \sqrt{\frac{9}{245}}B_{40}/B_{00}]} \quad (12)$$

TABLE I. Mössbauer parameters^a of HB ${}^{129}\text{IA}$, P ${}^{129}\text{IA}$, H ${}^{129}\text{INA}$, T₄, and D ${}^{129}\text{IT}$.

Compound	Temperature (K)	$e^2q^{127}Q^b$ (MHz)	${}^{129}\delta_{z\text{nTe}}$ (mm/sec)	Γ (mm/sec)	η
HB ${}^{129}\text{IA}$					
(a) Solid	4.2	-1815 ± 25	0.12 ± 0.04	0.84 ± 0.08	0.05 ± 0.03
(b) Frozen ethanol glass	4.2	-1835 ± 25	0.14 ± 0.04	0.85 ± 0.08	0.03 ± 0.03
(c) 20% concentration in HBPA	4.2	-1820 ± 25	0.13 ± 0.04	0.78 ± 0.08	0.06 ± 0.03
P ${}^{129}\text{IA}$	4.2	-1815 ± 25	0.14 ± 0.04	0.78 ± 0.08	0.04 ± 0.03
H ${}^{129}\text{INA}^c$	55	-1926 ± 14	0.110 ± 0.011	0.80 ± 0.08	0.10 ± 0.01
T ₄ ^d	4.2	-1954 ± 21	0.26 ± 0.03	0.84 ± 0.08	0.10 ± 0.03
D ${}^{129}\text{IT}^d$	4.2	-1950 ± 21	0.30 ± 0.03	0.82 ± 0.08	0.07 ± 0.03

^a The quoted errors include estimated systematic errors.

^b The values for ${}^{129}\text{I}$ were converted to those of ${}^{127}\text{I}$ using the ratio $e^2q^{129}Q/e^2q^{127}Q = 0.701$ (Ref. 28).

^c Reference 9.

^d Reference 27.

where $\alpha = \sqrt{5}/4(3\cos^2\theta_1 - 1)(3\cos^2\theta_2 - 1)$.

The MB samples were oriented several times as a function of θ_1 (see Fig. 3). The orientation procedure is described in Sec. II. MB spectra of samples measured one week after orientation were indistinguishable from those obtained immediately after orientation.

The \mathfrak{M} values obtained from the MB measurements (see Sec. IV) are plotted versus θ_1 in Fig. 8. The solid curve in the figure corresponds to a value of $\theta_2 = 50^\circ$ in Eq. (12). The estimated experimental error on θ_2 is $\pm 4^\circ$. Unfortunately, there are no x-ray measurements on HBPA. However, x-ray measurements¹⁵ on BEA, which has a structure similar to that of HBPA, yield a smectic-*H* tilt angle of 56.2° . Since the structure of HB¹²⁹I is very similar to that of HBPA and our value of θ_2 is similar to that of DeVries *et al.*¹⁵ for BEA, it is reasonable to assume that $\theta_2 = 50 \pm 4^\circ$ is a good indication of the smectic-*H* tilt angle in HBPA.

In addition to the measurements of the smectic-*H* tilt angle, ¹²⁹I MB spectroscopy can be extended to the study of rotational invariance in LC. Sub-

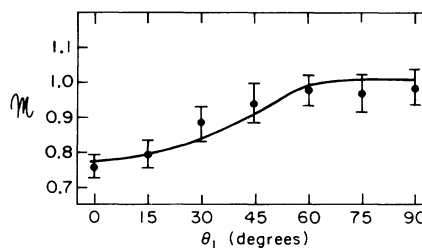


FIG. 8. A plot of the \mathfrak{M} values versus θ_1 .

stitution of the iodine to the ortho-position on the benzene ring allows one to probe rotational symmetry as well as the orientation of the long axis of the LC. In principle this method can be used to test McMillan's model of the smectic-*C* phase in which he postulated that the rotational freedom of the molecules about their long axis is frozen out. The methods and mathematical expressions presented in this paper can be applied to other ordered systems. One significant extension of this method would be the study of the orientation of ⁵⁷Fe-containing proteins in membranes.

*Work supported in part by the National Science Foundation under grant NSF GH 36966.

†Present address: Department of Physics, Princeton University, Princeton, N. J. 08540.

¹I. G. Chistyakov, *Usp. Fiz. Nauk* **89**, 563 (1966) [*Sov. Phys.-Usp.* **9**, 551 (1967)].

²R. M. Williams and D. Chapman, in *Progress in the Chemistry of Fats and Other Lipids*, edited by R. T. Holman (Pergamon, New York, 1970), pp. 3-74.

³G. W. Gray, *Molecular Structure and the Properties of Liquid Crystals* (Academic, New York, 1962).

⁴D. L. Ulrich, J. M. Wilson, and W. A. Resch, *Phys. Rev. Lett.* **24**, 355 (1970).

⁵V. I. Goldanskii, O. P. Kevdin, N. K. Kivrina, E. F. Makarov, V. Ya. Rochev, and R. A. Stukan, *Zh. Eksp. Teor. Fiz.* **63**, 2323 (1972) [*Sov. Phys.—JETP* **36**, 1226 (1973)].

⁶R. E. Detjen, D. L. Uhrich, and C. F. Sheley, *Phys. Lett.* **42A**, 522 (1973).

⁷J. M. Wilson and D. L. Uhrich, *Mol. Cryst. Liq. Cryst.* **13**, 85 (1971).

⁸D. L. Uhrich, Y. Y. Hsu, D. L. Fishel, and J. M. Wilson, *Mol. Cryst. Liq. Cryst.* **20**, 349 (1973).

⁹M. J. Potasek, E. Münck, J. L. Groves, and P. G. Debrunner, *Chem. Phys. Lett.* **15**, 55 (1972).

¹⁰G. W. Gray and B. Jones, *J. Chem. Soc.* 236 (1955).

¹¹M. J. Potasek (unpublished).

¹²W. Maier and A. Saupe, *Z. Naturforsch A* **15**, 287 (1960).

¹³K. K. Kobayashi, *Phys. Lett.* **31A**, 125 (1970).

¹⁴W. L. McMillan, *Phys. Rev. A* **4**, 1238 (1971).

¹⁵A. DeVries and D. L. Fishel, *Mol. Cryst. Liq. Cryst.* **16**, 311 (1972).

¹⁶R. J. Meyer and W. L. McMillan, *Phys. Rev. A* **9**, 899 (1974).

¹⁷W. L. McMillan, *Phys. Rev. A* **8**, 1921 (1973).

¹⁸M. E. Huth, Ph.D. thesis (Friedrichs Universität, 1909) (unpublished).

¹⁹A. E. Bradfield, K. J. P. Orton, and I. C. Roberts, *J. Chem. Soc.* 782 (1928).

²⁰M. H. Cohen and F. Reif, *Solid State Phys.* **5**, 321 (1957).

²¹P. G. Debrunner, in *Spectroscopic Approaches to Biomolecular Conformation*, edited by D. W. Urry, (Academic, New York, 1970), pp. 230, 223.

²²G. K. Shenoy and B. D. Dunlap, *Nucl. Instrum. Methods* **71**, 285 (1969).

²³V. I. Goldanskii and R. H. Herber, *Chemical Applications of Mössbauer Spectroscopy* (Academic, New York, 1968), pp. 104, 401.

²⁴B. L. Chrisman and T. A. Tumolillo, *Tech. Rept. No. 178* (University of Illinois, 1969) (unpublished).

²⁵J. L. Groves, Ph.D. thesis (University of Illinois, 1971) (unpublished).

²⁶W. L. McMillan (private communication).

²⁷J. L. Groves, M. J. Potasek, and G. DePasquali, *Phys. Lett.* **42A**, 493 (1973).

²⁸N. N. Greenwood and T. C. Gibb, *Mössbauer Spectroscopy* (Chapman and Hall, London, 1971), pp. 465-468.